21st Australasian Fluid Mechanics Conference
Adelaide, Australia
10-13 December 2018

Numerical Investigations of Flow Over a Confined Circular Cylinder

P. Mathupriya[1], L. Chan[2], H. Hasini[1], and A. Ooi[2]

[1]Department of Mechanical Engineering
Universiti Tenaga Nasional, Kajang 43000, Malaysia

[2]Department of Mechanical Engineering
University of Melbourne, Victoria 3010, Australia

Abstract

The unsteady flow over a cylinder confined by two parallel walls using direct numerical simulation (DNS) is investigated. The effects of two parameters, namely the Reynolds number and the blockage ratio, are the main focus for this study. The three-dimensional flow is simulated where the circular cylinder is placed symmetrically in a planar channel with a blockage ratio of $\beta = 0.5$ at $Re = 200$, 300 and 500. Quantitative analysis of the flow is conducted where the lift, C_L and drag coefficient, C_D and Strouhal number, S_t are investigated as β and Re are systematically varied. In the present study, it is found that different instability regimes are observed as the Re of the flow increases. The presence of a distinct shedding frequency is observed at $Re = 200$. However, increasing the Reynolds number further, the contribution of a range of frequencies surrounding the peak frequency appears as shown in the spectral analysis of the lift coefficient. The confinement effects played an important role in changing the properties of the wake. Counter rotating spanwise vortices are formed as a result of the interaction between the cylinder wake and the boundary layer of the walls in the channel which is entrained into the vortex street.

Introduction

The flow separation over bluff body is a classical problem in fluid mechanics as it is hard to predict the undesirable phenomena such as increment in drag, losses in the lift and the fluctuations in pressure field [1]. Research on flow over bluff bodies have also focused on heat transfer rates of the fluid using experimental and numerical techniques with the aim of improving thermal performance [2, 3]. These flows are commonly observed in cooling and heating systems such as heat exchangers in chemical and power plants. Most research on the flow over a bluff body is represented by a circular cylinder [2, 4]. The case of a bluff body confined by no-slip channel wall is less explored where it affects the instabilities in the wake of the flow over a confined cylinder. Current work is inspired by [5] where numerical study of the wall effects is carried out on two-dimensional flow around a circular cylinder over a wide range of blockage ratios ($\beta = D/H$ where D is the diameter of the cylinder and H is the height of the channel) from 0.1 to 0.9 and Re up to 280. They investigated the blockage ratio effects on the vortex shedding characteristics and presented the neutral curve and stability maps. The work is extended by [6] where a low frequency beating is observed when the confined cylinder is simulated with $Re = 300$ and $\beta = 0.5$. This low frequency beating is postulated to be the influence of the channel walls on the vortex shedding behind the cylinder. Three-dimensional flow over confined circular cylinder with blockage ratio of 0.2 and a Reynolds number range of 10-390 are investigated by [7]. Their results show the transition from 2-D to 3-D shedding flow regime that occurs at Re between 180 and 210. Besides, it also dominated by different instabilities which are mode A (discontinuous change in the wake formation), mode B (appearance of small-scale streamwise vortex structure) and vortex dislocations where it is similar to the case of an unconfined circular cylinder. In the present study, the simulation of three-dimensional flow for the blocked channel is conducted using DNS where the governing equation is solved without any modelling. The main objective of this study is to investigate the flow over a confined circular cylinder with a fixed blockage ratio while varying the Reynolds number. There is no published on the three-dimensional flow in a confined channel with fixed $\beta = 0.5$ in the Reynolds number range of 200 to 500.

Computational Setup

A 3-D incompressible flow over a cylinder symmetrically confined by two parallel walls is shown in figure 1. There are two different distances used at the streamwise length of the domain which are L_1 = -10 at the upstream and L_2 = 30 at the downstream of the cylinder. The height of the channel is fixed with a distance of $H = 2$. The diameter of the cylinder, D is determined based on $\beta = 0.5$. The width of the domain in spanwise direction is $W = 8D$. U_x is the inflow velocity. The x, y and z axis denotes the streamwise, wall-normal and spanwise directions respectively. The incompressible unsteady Navier-Stokes

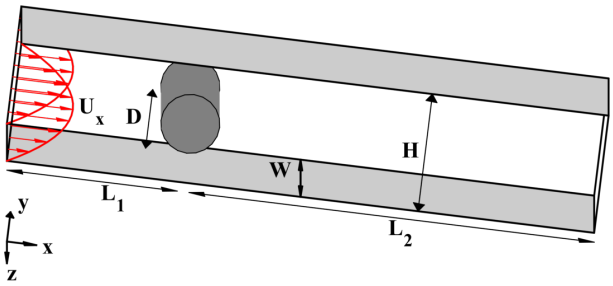

Figure 1: The sketch of the computational domain for a cylinder in a channel.

equations are defined in the following form:

$$\nabla \cdot \mathbf{u} = 0 \tag{1}$$

$$\frac{\partial \mathbf{u}}{\partial t} + (\mathbf{u} \cdot \nabla)\mathbf{u} = -\nabla p + \frac{1}{Re}\nabla^2 \mathbf{u} \tag{2}$$

where $\mathbf{u}$ represents the velocity vector, p is the pressure and Re is the Reynolds number, where it is defined as:

$$Re = \frac{U_{max} D}{\nu} \tag{3}$$

where U_{max} is the maximum value at inlet velocity and ν represents the kinematic viscosity. OpenFOAM (Open Field Operation and Manipulation) toolbox is used to conduct the DNS. OpenFOAM is an open source, finite volume CFD software that has been widely used by engineers and scientist for both commercial and academic purposes. The numerical simulations are

conducted using icoFoam solver which solves the incompressible Navier-Stokes equations using the PISO algorithm. The inlet velocity for the blocked channel follows the parabolic profile:

$$U_x = [1 - y^2] \tag{4}$$

No-slip boundary condition is imposed on the surface of the cylinder and the channel walls. In order to avoid distortion of flow structure leaving the domain at the outlet, a zero-gradient boundary condition is applied for velocity and a fixed value of 0 is applied for pressure. Slip boundary condition is applied to the spanwise boundaries. The second-order centred difference scheme is used for spatial discretization and the second-order backward differencing scheme used for time discretization. The computational domain contained a total of 3,039,000 cells and is simulated at Re = 200, 300 and 500 with β = 0.5. There are 200 cells around the circumference of the cylinder and 30 cells in the spanwise direction. There are 40 cells between the cylinder and the walls of the channel. A grid independence study has been conducted and the mean drag coefficient of the current mesh is identical with refined mesh. The mean lift coefficients for the current and refined mesh is also close to zero (5.74e-05 and 6.02e-05 respectively).

The initial condition of these simulations is mapped from the result of a steady simulation to achieve faster convergence. These simulations are then run for 500 U_{max}/D to achieve a statistically converged flow state. The forces acting on the confined cylinder are the drag and lift force. These forces are based on the integration of the shear stress and pressure along the surface of the cylinder. The dimensionless drag and lift coefficient are defined as:

$$C_L = \frac{F_L}{0.5{U_{max}}^2 D} \tag{5}$$

$$C_D = \frac{F_D}{0.5{U_{max}}^2 D} \tag{6}$$

The frequency of vortex shedding is identified based on Strouhal number which is written in the following form:

$$S_t = \frac{Df}{U_{max}} \tag{7}$$

where f is the period of vortex shedding which is calculated via spectral analysis of the time resolved lift coefficient of the cylinder. The equations presented in this paper are in non-dimensional form.

Results and Discussions

Vortex shedding that appeared in the three-dimensional blocked channel for β = 0.5 is initiated without forcing any external-flow disturbances. The time series of the lift and drag coefficient for β = 0.5 at Re = 200, 300 and 500 are presented in figures 2 and 3 respectively. The flow is unsteady and fluctuations in C_L is observed. The C_D also fluctuates but the magnitude of fluctuation is significantly smaller than C_L. The fluctuations in C_L and C_D increases as the Reynolds number increased. At Re = 200, the lift and drag coefficients are periodic and had reached a statistically stationary state. At Re = 300, the transient period length is particular long approaching 100 time units indicating unsteady state of the wake. The length of transient period became shorter as the Reynolds number increased. For the case of Re = 500, the transient period is approximately 80 time units indicating the wake from the unsteady structure. This behaviour showed that the quasi-steady flow phase reduces as the Reynolds number increases. The time-averaged force coefficients for each of these cases are tabulated in table 2. The mean value of lift and drag coefficients are obtained from the time taken by the periodic behavior of the force coefficient in unsteady state, where

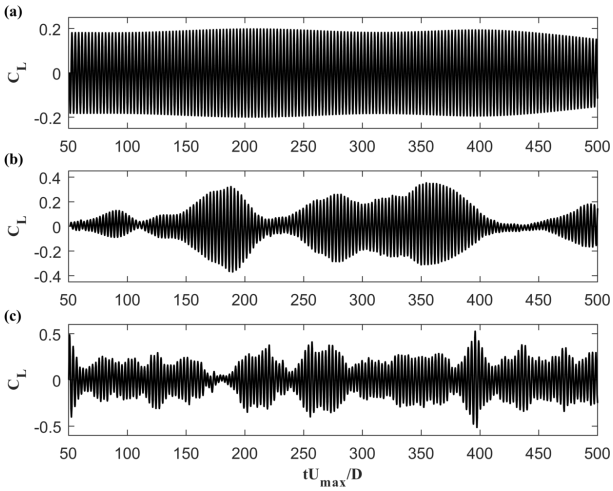

Figure 2: Lift coefficient time histories for the three-dimensional cases at Re = (a) 200, (b) 300, and (c) 500.

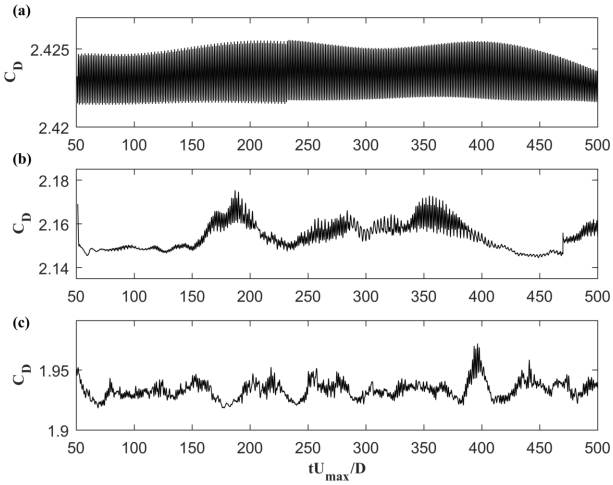

Figure 3: Drag coefficient time histories for the three-dimensional cases at Re = (a) 200, (b) 300, and (c) 500.

the time-averaged is taken from dimensionless time units which are 50 - 500 tU_{max}/D. The values of lift and drag coefficient will be changed if the simulation ran for a longer period. The $\overline{C_L}$ value increases as the Reynolds number increased at the range of 200 to 500. The $\overline{C_L}$ value is very close to zero with varied Reynolds number if the time-averaged is long enough. $\overline{C_D}$ decreases as the Reynolds number increased because the center of low pressure flows into downstream, similar to the observations of [8]. This causes the suction effect on the cylinder to be reduced based on the flow direction.

The period of the vortex shedding is determined by conducting a spectral analysis on the fluctuations of the lift coefficient. The plot shown in figure 4 indicates the dominant frequencies in the fluctuations of the lift coefficients. In figure 4(a), the oscillations in lift coefficient is periodic and is dominated by a single frequency with S_t = 0.349 at Re = 200. This is due to the periodic shedding of vortices in the wake of the cylinder. The current result of S_t in three-dimensional blocked channel is compared with the frequency of 2-D simulation from [5] with the same parameters and configuration which had S_t = 0.3513. Current three-dimensional simulation agrees well with the two-dimensional data of [5] and has a small Strouhal number deviation of approximately 0.6%. Based on the plot in figure 4(b),

Case	Re	$\overline{C_L}$	$\overline{C_D}$
Case 1	200	-5.9634e-04	2.4234
Case 2	300	0.0010	2.1540
Case 3	500	0.0014	1.9331

Table 1: The time-averaged lift and drag coefficient for Re = 200, 300 and 500.

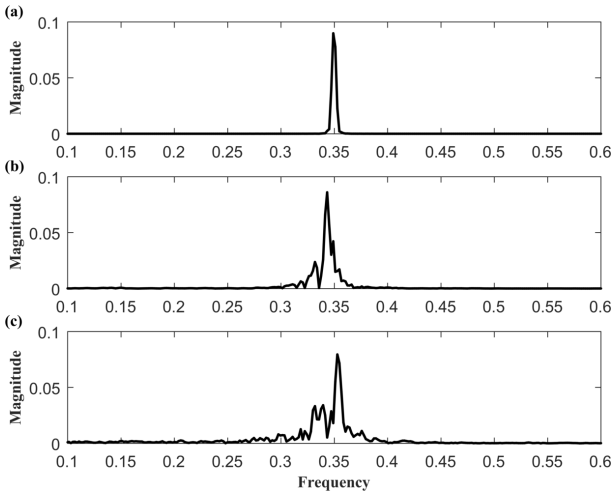

Figure 4: The spectral analysis for the three-dimensional cases at Re = (a) 200, (b) 300, and (c) 500.

two dominant frequencies are observed at 0.3319 and 0.3433 at Re = 300. These frequencies correspond to the double beating and differs with the 2-D simulation from [7] which had frequencies of 0.513 and 0.468. In figure 4(c), three distinct frequencies appeared at Re = 500, at f = 0.3319, 0.3395, and 0.3529. The number of frequencies increases as Reynolds number increases. The confined wall from the blocked channel may cause the distinct frequencies as a result of the interaction on the wall of the channel, as the vortices interact the wall at higher Re.

The spanwise vortices can be observed when the flow separates from the surface of the cylinder. Generally, the vorticity magnitude is applied to identify the structures of these vortices. However, this method failed to identify the vortices near the channel walls and unable to differentiate between swirling motion and shear. Therefore, λ_2 vortex criterion method is used to detect the vortical motion in this three-dimensional simulations [9]. This iso-surfaces of λ_2 highlights the swirling motion and the vortices in the flow. The different instabilities in the wake of the three-dimensional blocked channel with varied Reynolds number are shown in figures 5, 6, and 7. The spanwise wake of the vortex cores is observed to shed from confined cylinder at Re = 200 in figures 5(a-c). The trajectories of the vortices shedding at the top of the cylinder, which have negative spanwise vorticity, are transported to the bottom wall of the channel as it advects downstream and vice-versa for the vortices shedding at the bottom of the cylinder. This periodic shedding is known as the reverse Von Kármán vortex street.

The confinement effects may cause the counter rotating spanwise vortices to appear. This is due to the interaction with the lateral walls that is entrained into the vortex street. The breakdown of vortex cores depicted by iso-surfaces λ_2 is separated by three periods at Re = 300 and 500 in figures 6 and 7. The iso-surfaces are colored by spanwise vorticity component to have a clearer view on spanwise vortex core. The negative vortex roller which is blue at the top of the cylinder started to break approximately at x/D = 6 as shown in figure 6(a). At approxi-

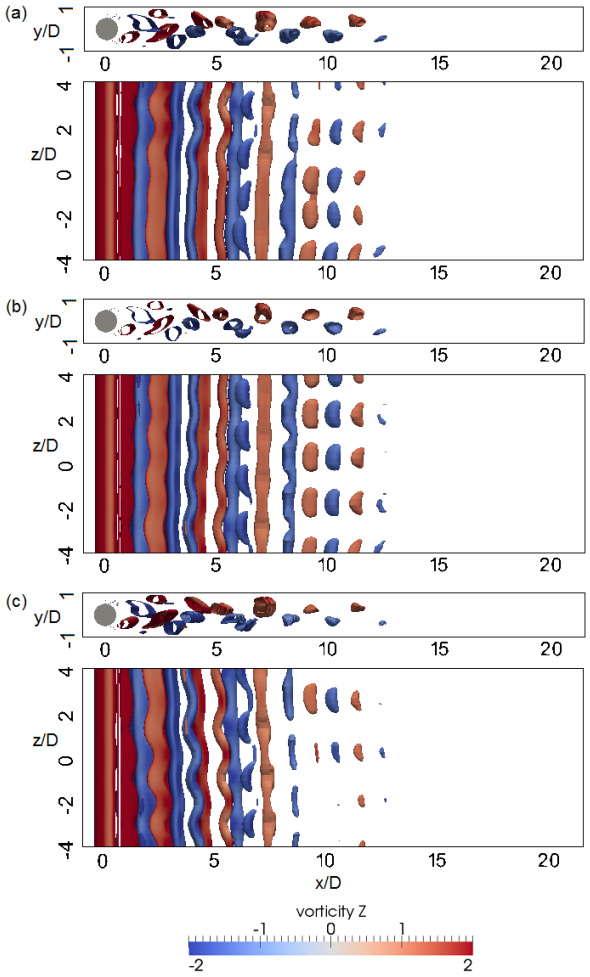

Figure 5: Iso-surfaces of λ_2 with threshold of 0.0015Re for Re = 200 and β = 0.5, coloured by the spanwise vorticity component at t = (a) 300 D/U_{max}, (b) 400 D/U_{max}, and (c) 500 D/U_{max}.

mately x/D = 8 in figures 6(b) and (c), both positive and negative vortex roller lost its spanwise continuity and break into smaller structures. The negative vortex roller started losing its continuity approximately at x/D = 4 in figure 7(a). In figures 7(b) and (c), the vortex cores broke into smaller pieces when the x/D reached approximately x/D = 9. The streamwise vorticity did not appear in any simulation cases, unlike in [7]. This is because the distance between the cylinder and the lateral wall is far as the blockage ratio in [7] is β = 0.2. Since the blockage ratio of current simulations of a confined cylinder is β = 0.5, the close proximity with the lateral walls of the channel may have suppressed these streamwise structures. The breakdown of the vortex cores occurs at an earlier downstream location when the Reynolds number increases, similar to the observations of [7].

Conclusions

The three-dimensional flow over a blocked channel has been performed using direct numerical simulations (DNS). The blockage ratio is kept constant at β = 0.5 and Re = 200, 300 and 500. The time series for the lift and drag coefficient are analysed. The frequency of the vortex shedding is identified through spectral analysis based on the fluctuations of the lift coefficient. At higher Reynolds number, a large spread of frequencies are observed in the spectral plot of the lift coefficient. The λ_2 vortex criterion method is used to visualise the structures

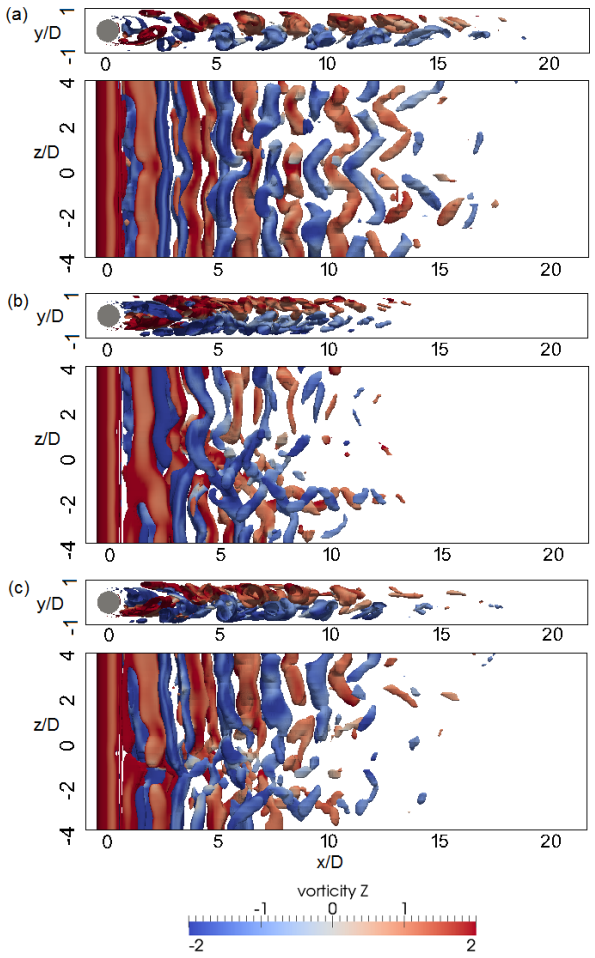

Figure 6: Iso-surfaces of λ_2 with threshold of $0.001Re$ for Re = 300 and $\beta = 0.5$, coloured by the spanwise vorticity component at t = (a) 300 D/U_{max}, (b) 400 D/U_{max}, and (c) 500 D/U_{max}.

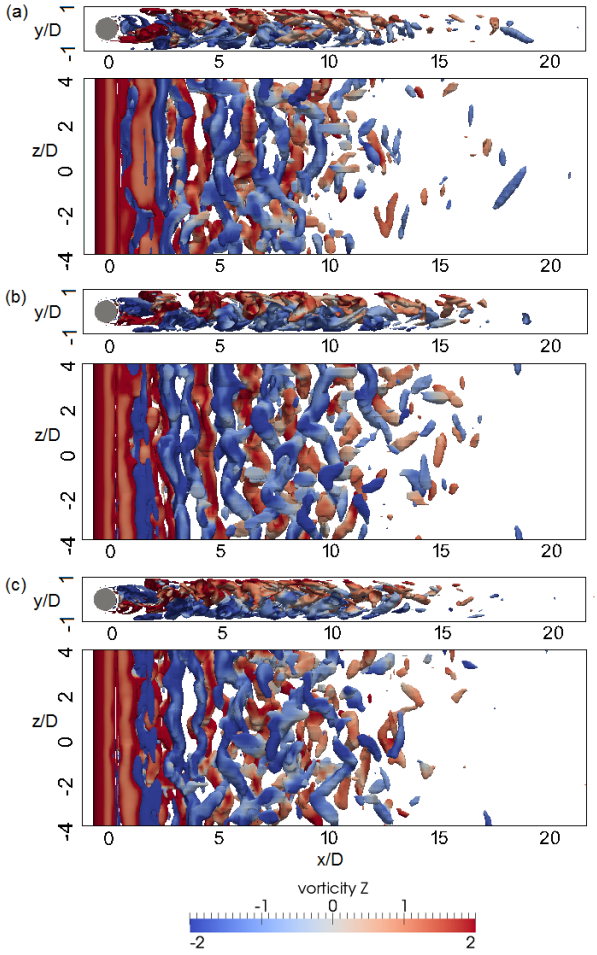

Figure 7: Iso-surfaces of λ_2 with threshold of $0.0006Re$ for Re = 500 and $\beta = 0.5$, coloured by the spanwise vorticity component at t = (a) 300 D/U_{max}, (b) 400 D/U_{max}, and (c) 500 D/U_{max}.

in the flow. The breakdown of vortex cores can be observed at an earlier downstream location at higher Reynolds number. The confinement effects cause the appearances of counter rotating spanwise vortices, and suppresses the formation of streamwise vortices.

Acknowledgements

The financial assistance received from UNITEN BOLD scholarship and UNITEN BOLD internal grant is greatly appreciated.

References

[1] C. H. Yen, U. J. Hui, Y. Y. We, A. Sadikin, N. Nordin, I. Taib, K. Abdullah, A. N. Mohammed, A. Sapit, and M. A. Razali, Numerical study of flow past a solid sphere at high Reynolds number, *IOP Conf. Series: Materials Science and Engineering*, **243**, 2017, 012042.

[2] M. I. Yuce, and D. A. Kareem, A numerical analysis of fluid flow around circular and square cylinders, *Am. Water Works Assoc.*, **108**, 2016, 546–554.

[3] P. Moin, and K. Mahesh, Direct numerical simulation: a tool in turbulence research, *Annu. Rev. Fluid Mech.*, **30**, 1998, 539–578.

[4] L. Zovatto, and G. Pedrizzetti, Flow about a circular cylinder between parallel walls, *J. Fluid Mech.*, **440**, 2001, 1–25.

[5] M. Sahin, and R. G. Owens, A numerical investigation of wall effects up to high blockage ratios on two-dimensional flow past a confined circular cylinder, *Phys. Fluids*, **16**, 2004, 1305–1320.

[6] M. D. Griffith, J. Leontini, M. C. Thompson, and K. Hourigan, Vortex shedding and three-dimensional behaviour of flow past a cylinder confined in a channel, *J. Fluids Struct.*, **27**, 2011, 855–860.

[7] N. Kanaris, D. Grigoriadis, and S. Kassinos, Three dimensional flow around a circular cylinder confined in a plane channel, *Phys. Fluids*, **23**, 2011, 064106.

[8] W. Gao, D. Nelias, Y. Lyu, and N. Boisson, Numerical investigations on drag coefficient of circular cylinder with two free ends in roller bearings, *Tribology International*, **123**, 2018, 43–49.

[9] J. Jeong, and F. Hussain, On the identification of a vortex, *J. Fluid Mech.*, **285**, 1995, 69–94.